ChemPubSoc Europe

DOI: 10.1002/cphc.201800509

CHEMPHYSCHEM Communications

Practical Guidelines for Shell-Isolated Nanoparticle-Enhanced Raman Spectroscopy of Heterogeneous Catalysts

Thomas Hartman,[a] Caterina S. Wondergem,[a] and Bert M. Weckhuysen*[a]

Shell-isolated nanoparticle-enhanced Raman spectroscopy (SHINERS) has proven to be a useful characterization tool for heterogeneous catalysis research. The advantage of SHINERS lies in studying surface reactions on solid catalysts, including the detection of reactants, intermediates and products, in real time. However, due to the extremely strong local electric fields, minor amounts of contaminants can already have a big impact on the quality and interpretation of the spectroscopic data obtained. Often, a large part of the organic fingerprint region (1100–1700 cm^{-1}) is omitted from SHINER spectra as this is not the main region of interest. However, we show that bands in this region are an important indication of the cleanliness of the substrate. In this work, we propose robust synthesis and measurement protocols to obtain clean SHINERS substrates amenable for catalysis research. By cleaning the substrates with various heat and oxidation treatments, featureless Raman spectra can be obtained. Furthermore, very pure gas feeds are required and must be obtained by flushing the gas lines and the reaction chamber beforehand and installing a filter for further cleaning the gas feed. Controlling the laser power to limit substrate and sample degradation is also a crucial aspect of proper measurement protocols.

Surface-enhanced Raman spectroscopy (SERS) has the ultimate potential to elucidate molecular structures in single-molecule events.[1] Raman spectroscopy is already a strong complementary technique to IR spectroscopy as it can probe vibrations of molecules and materials over a wider energy range,[2] but in the case for SERS, this spectroscopic technique even becomes a strong surface characterization tool for *in situ* studies of heterogeneous catalysts.[3–5] SERS has been implemented for the study of surface-reactions since its invention,[6–9] which has led to the discovery of various reaction pathways for chemical reactions, including possible intermediates.[10–14] In SERS, noble metal nanostructures with plasmonic properties are applied for the enhancement of the Raman signal. The conduction electrons at the surface of these nanostructures can resonate with the excitation laser wavelength and across the Stokes frequency, resulting in a strong enhancement of the incident light and the scattered light within nanometers of the metal surface.[15] To extend the applicability of SERS, metal overlayers were first prepared over existing Au or Ag surfaces.[16,17] Later, shell-isolated nanoparticle-enhanced Raman spectroscopy (SHINERS) was developed to create a more universal technique.[18] When the plasmonic nanoparticles (NPs) are coated with a dielectric layer, such as SiO_2, the technique can be regarded as a non-invasive characterization tool to study virtually any substrate.[19] In our group, SiO_2- and TiO_2-shell-isolated nanoparticles (SHINs) were recently applied to study hydrogenation catalysis over a range of metals.[20]

Since SERS and SHINERS are extremely sensitive techniques, contamination of the sample can have a large impact on spectral interpretation. Amorphous carbon is one of the most common contaminants, and was identified as the "bottle-neck" for SERS to be widely applied.[21] Organic residues will be present as a result of the preparation conditions and can be decomposed to form amorphous carbon under the conditions generated by the excitation of the plasmonic nanostructures. Depending on the nature of the plasmonic nanostructures, such conditions are perceived as heating,[22] hot-electron injection[4] or degradation by strong electromagnetic effects.[23] Because coke species have a large Raman scattering cross-section, even a small amount can result in intense signals between 1200–1700 cm^{-1}, with the typical 1350 cm^{-1} disordered (D) carbon band and 1600 cm^{-1} graphitic (G) carbon band as the strongest interference. More problematic is that SERS and SHINERS can detect local changes in amorphous carbon as blinking spectra with fluctuating spectral intensities and band locations. The random location of these peaks make them difficult to subtract or ignore.[21] Such problems were already observed in the application of SERS for the study of CO hydrogenation over Rh in the 1990s. At elevated temperatures in the absence of oxygen, Weaver *et al.* observed the conversion of organics to coke species over the SERS substrates, resulting in features that obscured the spectra in the 1200–1600 cm^{-1} range.[12,24] This range was therefore left out of the interpretation. Additionally, the presence of carbon affects the performance of a catalyst as it can block access to the reactive surface and its formation should therefore be prevented.[25]

Because the field of SHINERS in heterogeneous catalysis is relatively new, the information on sample preparation is scarce in the literature and remains often limited to some brief discussions in the experimental section of these articles. We have therefore worked on the development of a valuable set of practical guidelines to inform the scientific community about the possible routes to tackle substrate and spectral contami-

[a] *T. Hartman, C. S. Wondergem, B. M. Weckhuysen*
Inorganic Chemistry and Catalysis
Debye Institute for Nanomaterials Science, Utrecht University
Universiteitsweg 99, 3584 CG Utrecht, (The Netherlands).
E-mail: b.m.weckhuysen@uu.nl

Supporting information for this article is available on the WWW under https://doi.org/10.1002/cphc.201800509

nation. Using these guidelines, the reproducibility of *in situ* experiments is guaranteed, which is a necessity for SHINERS to become a more routine technique in the field of catalysis. Three pretreatments to remove organic residues were investigated in this work; a heat treatment in air up to 300 °C, oxidation by UV/O_3 at room temperature and a reduction treatment up to 250 °C in H_2. Furthermore, the purity of the gas feed was found to be critical and can be improved easily with a filter. It was found that minor contaminations in the gas feed caused by impurities have a major effect on the SHINERS spectral interpretation as well as on the catalyst properties. Finally, the guidelines are applied to Ru/Au@TiO_2 and Ru/Ag@SiO_2 SHINs to demonstrate the universality of the methods proposed.

Catalytically active SHINERS substrates were prepared that enhance the Raman signal with a factor of over 10^4.[20] First, small Au seeds of 16 nm were prepared and further grown to 80 nm with $HAuCl_4$, using hydroxylamine hydrochloride as reducing agent.[26] A silica coating of 2 nm was grown over the Au cores using (3-aminopropyl)trimethoxysilane (APTMS) and sodium silicate in water at 90 °C for 40 min.[27] When dried and aggregated over Si wafers, these nanostructures were found to be optimal for enhancing the Raman scattering with a 785 nm laser connected to our Raman microscope.[20] Finally, catalyst precursors were assembled over the SHINs by mixing aqueous $RuCl_3$ and Au@SiO_2 SHINs, followed by drying on a Si wafer. A visual inspection of the steps involved in the synthesis was performed with transmission electron microscopy (TEM), as shown in Figure 1a–e. The complete details of the preparation can be found in the Supporting Information (SI). The coating thickness of the SHINs is essential to control; our previous work demonstrated that a coating of minimally 2 nm is required for stable SHINERS signals under elevated temperatures.[20] However, when the isolating shell reaches 3 nm, the signal is strongly diminished and becomes unsuitable for *in situ* measurements.

Organic residues are inherent to colloidal synthesis, because the controlled growth of nanoparticles requires several types of directing agents.[28] Therefore, the colloidal products were cleaned by three consecutive centrifugation and washing steps with purified water (demineralized milli-Q, 18.2 MΩ·cm resistivity). Although with thermogravimetric analysis (TGA) no mass loss was observed over 20–800 °C (Figure S1 in the Supporting Information), organics are still observed in the SHINER spectra of two untreated samples, as illustrated in Figure 1f. Even after several washing steps, a fraction of the molecules remains on the surface and will influence the observed SHINER spectra. The spectra of untreated SHINER substrates vary not only between different samples, but even over different spots within a single sample. The catalyst precursor was then activated by a reduction step in H_2 at 250 °C for 1 h in Figure 1g. When the contaminants were not removed, broad features of carbon remain, obscuring the spectra. The substrates can be used for the detection of adsorbed carbonyls with ν(Ru-CO) at 480 cm^{-1} and ν(RuC–O) at 2000 cm^{-1} in Figure 1h. However, the study of adsorbed reactants and products becomes difficult due to the strong features between 1100–1700 cm^{-1} originating from organics. This region is often not measured as the main focus is the metal-adsorbate interactions, with as added benefit a reduced acquisition time. When this spectral region is omitted, important information is excluded from interpretation, as it can be used to evaluate the cleanliness of the sample (Figure S2). For example, when contamination is more substantial, the deposited carbon can isolate the catalyst from reactants, blocking CO from adsorbing on surfaces. This was observed in the case of CO adsorption on Ru that was heavily contaminated. The substrate was required to be heated to 300 °C in synthesis gas (2 H_2:1 CO) before CO adsorption was visible

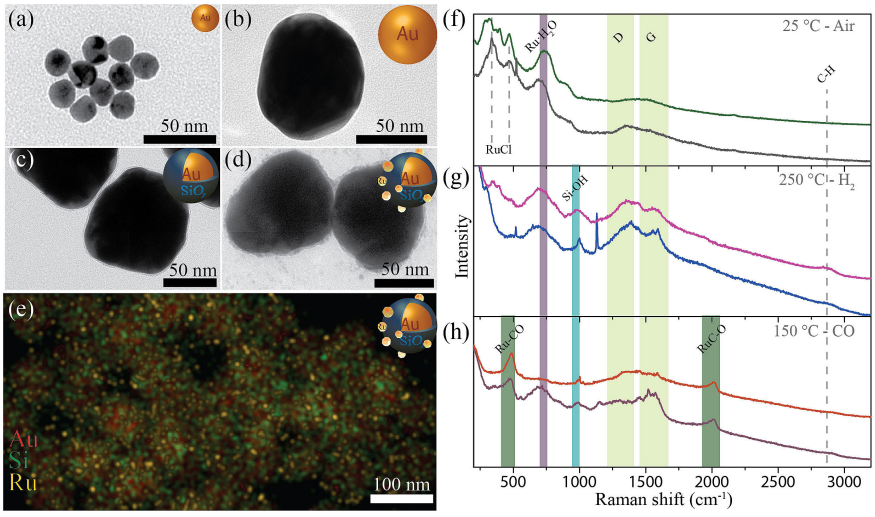

Figure 1. TEM and STEM-EDX microscopy images of the synthesis steps involved to prepare Ru/Au@SiO_2 based SHINs: **(a)** Au seeds of 16 nm; **(b)** Au nanoparticles (NP) of 80 nm; (c) SiO_2-SHIN of 80 nm with 2 nm SiO_2 shell; **(d)** Ru catalysts assembled over SiO_2-SHINS after reduction at 150 °C in H_2; **(e)** STEM-EDX image of Ru catalysts assembled over SiO_2-SHINS after reduction at 150 °C in H_2 with Au indicated with red, Si with green, and Ru with yellow. **(f)** *In situ* SHINER spectra of two separate substrates of untreated $RuCl_3$/Au@SiO_2 as obtained after synthesis; **(g)** followed by reduction to Ru/Au@SiO_2 under H_2 at 250 °C; and **(g)** after CO adsorption at 150 °C [785 nm, 0.81 mW, 10 s].

(Figure S3). This result further demonstrates the need to remove residual organics before catalysis with robust cleaning methods, and that the fingerprint region needs to be included in the analysis to verify the cleanliness.

The contaminants before any treatment are identified as organics in Figure 2a, with δ_{as}(CH) at 1440 cm^{-1} and $\nu_s(CO_2^-)$ and $\nu_{as}(CO_2^-)$ of organic carboxylic acid salts at 1340 and 1560 cm^{-1}, respectively, most likely from remaining citrates.[29,30] The substrates therefore have to be cleaned prior to *in situ* SHINERS experiments. In contrast to SERS substrates,[24] Au@-SiO_2 NPs can withstand strong oxidation treatments to remove organic residues without sacrificing the Raman signal enhancing properties, as demonstrated in Figure 2a.[20] Using UV/O_3 for 1 h, all observable organic contaminants can be removed without affecting the $RuCl_3$ spectrum. In addition, heat treatments in air at 200 °C and 300 °C for 1 h will remove all organics and will also oxidize $RuCl_3$ to RuO_2, as is apparent from the intense Raman bands between 100–700 cm^{-1}. The bands observed in this work are much broader than conventional Raman experiments of RuO_2. Although it is known that Raman bands of nano-sized RuO_2 broaden and red-shift with respect to bulk RuO_2 Raman bands at 528, 644 and 716 cm^{-1},[31] hardly any separate bands are detected here with SHINERS. Because of its highly localized sensitivity, SHINERS probes the RuO_2–SiO_2 interface of NPs in the range of 3 nm, and therefore, more strain is observed in comparison to conventional Raman.[32,33] Two contamination bands remained after the cleaning procedures at 1050 cm^{-1} and 2130–2150 cm^{-1}. They are not related to organic contaminations, but can be ascribed to adsorbed NO_x impurities originating from the atmosphere.[34,35] Nitrates adsorbed in a bridged or bidentate conformation result in features expected at 1050 cm^{-1}. The peak at 2140 cm^{-1} indicates the presence of triple bonded C≡C or C≡N stretching vibrations of adsorbed alkynes or nitriles.

To obtain active hydrogenation catalysts, it is necessary to reduce Ru^{x+} catalyst precursors to metallic Ru^0. The reduction of Ru^{x+} species occurs at temperatures above 150 °C under H_2 atmosphere.[20] After 30 min at 250 °C under 10 mL/min H_2 in 40 mL/min Ar flow all bands associated with RuO_2 or $RuCl_x$ disappeared, indicating the full reduction of the catalyst. The remaining Raman bands are associated with Si–OH (990 cm^{-1}) and Si (520 cm^{-1}) from the Si wafer.[36] However, in contrast to other work,[3] we observed the growth of carbon during the reduction. The major contribution to the SHINER spectra consists of carbonaceous species as is apparent by the carbon D and G bands at respectively 1350 and 1590 cm^{-1} (Figure 2b). The bands (re)appeared after reducing samples that were pretreated with UV/O_3 and heat treatment at 200 °C. Furthermore, the presence of other organic materials with δ_{as}(CH) at 1440 cm^{-1} and $\nu_s(CO_2^-)$ and $\nu_{as}(CO_2^-)$ of organic carboxylate acid salts at 1340 and 1560 cm^{-1} reappeared in the samples treated by UV/O_3. UV/O_3 treatments are therefore not completely effective for cleaning, as the contaminants seem to be of a similar origin as for untreated samples. Heat-treated substrates, in contrast to UV/O_3-treated samples, do not show the reappearance of organic species. However, the appearance of carbon was still observed. Organic molecules in the gas lines and reaction chamber are the most likely cause. Since the substrates appeared clean prior to reduction, the contamination must come from the reduction treatment. It is therefore important to add an extended flushing period before reduction, to remove any residual organics in the reaction chamber or gas lines. The growth of carbon can be prevented by flushing with the reaction gases for at least 15 min.

Before *in situ* SHINERS experiments we are therefore required to follow two important steps: cleaning the substrate and cleaning the gas feed. These two steps can be optimally combined by cleaning the substrate in the reaction chamber. In this manner, we can assure that the complete reaction chamber is clean, and simultaneously evaluate whether the sample is indeed clean. First, all the gas lines were flushed and then the sample was heated with 3–5 °C/min to 300 °C for 30 min to remove organic molecules. After cooling down to room temperature, the flow was changed to 10 mL/min H_2 in 40 mL/

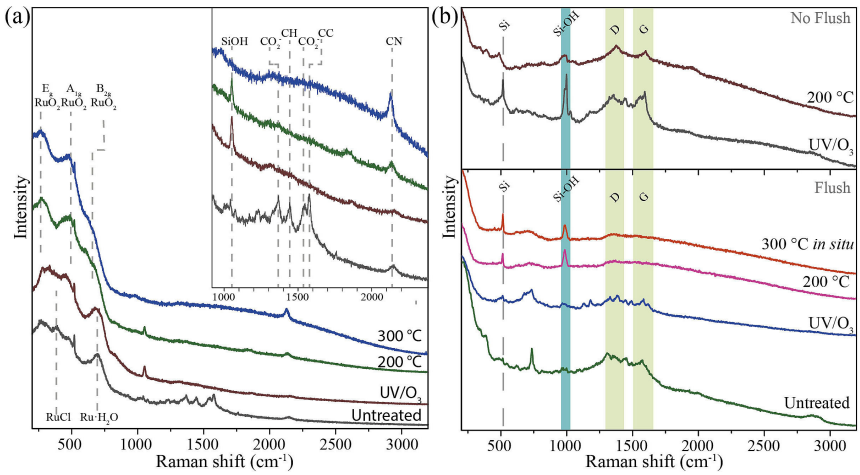

Figure 2. SHINER spectra of **(a)** $RuCl_3$/Au@SiO_2 in ambient conditions after heat treatment in air at 300 °C, 200 °C after UV/O_3 treatment, and an untreated substrate; **(b)** Ru^0/Au@SiO_2 after the pretreatments and a subsequent reduction step under H_2 at 250 °C. The top spectra were obtained when the reduction was performed without flushing, the bottom spectra were obtained after an extended flushing step of all gases for 15 min or longer. [785 nm, 0.81 mW, 10 s]

min Ar to reduce the RuO_2 at 250 °C for 30 min. The heating ramp should be limited to 5 °C/min, because faster heating rates will result in signal losses, most likely as a result of changes in the nanostructures, such as sintering of the catalyst particles.[37]

Clean substrates can now be implemented to study catalytically relevant conditions, such as the Fischer-Tropsch reaction. When opening the reaction chamber to CO, carbonyls will adsorb to the Ru surface, which is observed in the SHINER spectrum as linearly adsorbed CO with ν(Ru–C) at 480 cm^{-1} and ν(RuC–O) at 2000 cm^{-1}.[38–40] However, over extended measurements of 1 h at 200 °C or higher, strong bands in the D and G region of carbon accumulated, together with the growth of various bands around the M–C and C–O stretching vibrations (Figure 3a). The strong bands around 1300 and 1540 cm^{-1} indicate the presence of carbon species. Because their positions in the Raman spectrum are shifted, these species are of a different origin than the previously observed coke bands in Figure 2 and relate to more disordered graphite.[41] Furthermore, from 380–430 cm^{-1}, the Raman scattering bands of ν(Fe–CO) and ν(Ni–CO) are observed, between 500–800 cm^{-1} we observe δ(Ni–C–O) and δ(Fe–C–O) and between 1880–2200 cm^{-1} various ν(MC–O) stretching vibrations.[42–44] CO is stored in stainless steel and will therefore carry iron and nickel carbonyls.[45] We therefore assign the Raman bands around 2000 cm^{-1} to the C–O stretching vibrations of Ni and Fe carbonyls that have adsorbed to the SHINs. To prevent contamination by gas phase impurities, a filter was constructed of ZnO, γ-Al_2O_3, and activated carbon in that specific order to capture respectively H_2O, carbonyls, and organics. A microfilter was added to prevent microparticles from entering. When the filter is applied, *in situ* SHINERS studies of CO hydrogenation can be performed up to temperatures of 350 °C without the appearance of carbon species (Figure 3b).

To verify the reproducibility and signal stability of the SHINERS substrates under the cleaning procedures, two additional experiments were performed on four substrates. Of the four substrates, two substrates were cleaned with a heat treatment at 300 °C and the other two were used without any treatment. 40 random spots were then measured for their Raman signal intensity of ν(Ru-CO) (Figure S4). The SHINERS signal intensity of this band was found to be uninfluenced by the pretreatments. However, the reproducibility of the Raman spectra was significantly improved upon cleaning, with no spurious bands. Furthermore, after a hydrogen treatment, all random spots were found to be clear of organic contaminants in the fingerprint region, whereas the untreated samples were clearly not (Figure S5).

We have mainly focused on contamination bands until now, and a number of bands in the previously discussed spectra were left unassigned. These 'spectral contaminants' originate from the Au@SiO_2 substrate. The amorphous SiO_2 restructures as a result of the increased temperature. To understand the changes in the background, clean Au@SiO_2 substrates were subjected to the same reducing conditions as Ru/Au@SiO_2 in Figure 3c. The SHINER spectra of Au@SiO_2 and Ru/Au@SiO_2 are very similar, as is expected because metallic Ru does not have Raman bands in the observed region. After reduction, a broad feature at 480 cm^{-1} and a band is observed at 988 cm^{-1}. The 480 cm^{-1} band is associated with the R (symmetric stretching mode of the bridging oxygens between two Si atoms) and D_1 band (4-membered ring breathing mode). The band at 988 cm^{-1} is associated with terminal Si–OH stretching vibration. Heating further to 250 and 300 °C intensifies the bands, and additional bands appear at 630, 800 and 1055 cm^{-1}, that

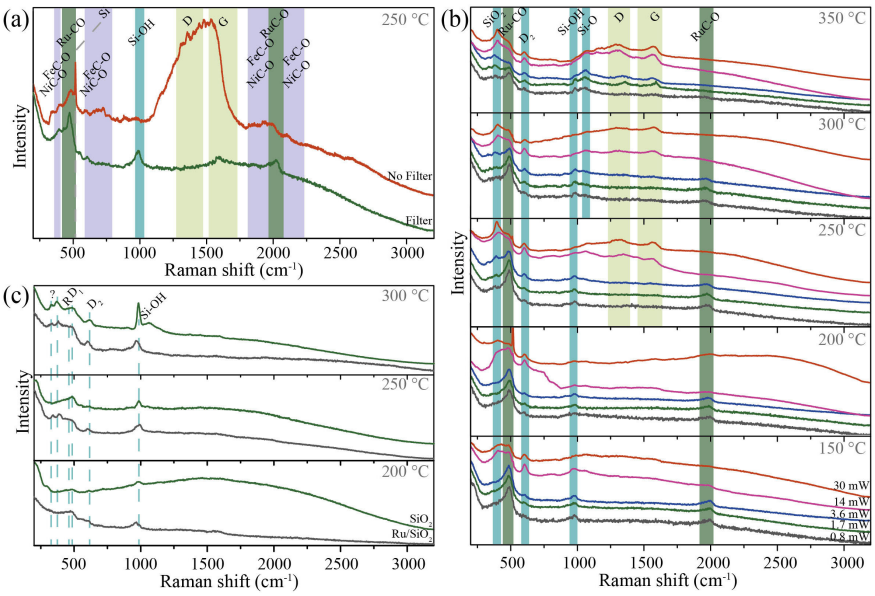

Figure 3. *In situ* SHINER spectra of Ru/Au@SiO_2 **(a)** Ru/Au@SiO_2 at 250 °C under CO-rich atmosphere with and without the filter consisting of ZnO, γ-Al_2O_3, activated carbon and a microfilter; **(b)** Ru/Au@SiO_2 under FTR conditions (10:20 CO:H_2) at 150–350 °C under changing laser power (0.8, 1.7, 3.6, 14 and 30 mW) **(c)** SHINER spectra of Au@SiO_2 (green) and Ru/Au@SiO_2 (grey) at 200, 250, 300 °C in a H_2-rich atmosphere.

originate from D_2 (3-membered ring breathing mode) and Si–O–Si bond bending, that correspond to bulk SiO_2 studies.[46] These bands were also observed after oxidation in air at temperatures up to 500 °C (Figure S6, however, in reducing environments with H_2, the SiO_2 transformation occurs already at 250 °C, and additional bands appear at 335 and 380 cm^{-1} that grow in intensity with the temperature (Figure 3c).

In Raman spectroscopy, the effect of the laser power on the sample can be problematic. Stronger laser power results in stronger signals, but chances of sample degradation increase. In SERS and SHINERS, the sample and the substrate can both be affected by the strong electromagnetic field. Furthermore, the nanoparticles can create heat and hot electrons to further complicate the effect of the light intensity.[4,22,23] It is therefore important to know the practical limits of laser power before substrate degradation occurs. In Figure 3b, the effect of laser power was investigated under CO hydrogenation at different temperatures. The laser power was regulated in a step-wise fashion with discrete filters that allowed control of the total transmission of the light before the sample. Under all the investigated temperatures, increasing the laser power results in a decrease in the intensity of the *v*(Ru–-CO) and *v*(RuC–O) stretching vibrations, the appearance of the D_2 band of SiO_2, and an increase in the unknown SiO_2 bands at 335 and 380 cm^{-1}. Increasing the temperature results in a lower threshold power for the laser to induce the spectral changes. At 150 °C, the SHINER spectrum is affected from 14 mW and higher, whereas at 250 °C the changes are detected already under 3.6 mW, and at 350 °C the changes are detected with 1.7 mW laser power. The effect of the 785 nm laser is therefore limited to heating of the substrate. The related laser power density can be found in Table S1.

By following the mentioned guidelines, clean SHINERS substrates are obtained that are ready to use for heterogeneous catalysis. These methods are robust and reliable for study of various solid catalysts over different SHINERS substrates. In fact, clean Au@TiO_2 (Figure S7) and Ag@SiO_2 (Figure S8) can also be obtained using the same methods. By following our guidelines – after flushing the reaction chamber and gas lines, an *in situ* calcination at 300 °C and by applying the filter – clean SHINER spectra were obtained on Ag@SiO_2 under both 532 and 785 nm laser excitation (Figure 4a). As expected, with a 532 nm excitation wavelength, we observe a stronger Raman signal. This can be related, first of all, to the Raman intensity depending on the excitation wavelength with λ^{-4}.[47] Furthermore, Ag-based SHINs have a stronger plasmon resonance with light in the 400–600 nm range (Figure S9) and because of the higher quantum efficiency of the CCD detector for 532 nm lasers, the Raman intensity in the higher wavenumber range is more intense. This results in a relatively stronger *v*(RuC–O) under CO hydrogenation conditions than observed with a 785 nm laser (Figure 4a). The background of fully reduced Ru/Ag@SiO_2 after complete hydrogenation of CO at 300 °C shows the same bands as for Ru/Au@SiO_2 with different relative intensities (Figure 4b). An advantage of implementing Ag plasmonic cores is that the stronger Raman signal intensity allows shorter acquisition times so that reactions can be followed with shorter intervals. However, because of the stronger plasmon resonance, the chance increases for degradation of the substrate and adsorbates due to thermal or electromagnetic effects. The threshold for laser induced damage is observed at 160 μW under CO hydrogenation conditions over Ru/Ag@SiO_2 (Figure 4c). Under methanation conditions (50 mL/min H_2 and 5 mL/min CO at 210 °C), the *v*(Ru-CO) and *v*(RuC–O) of linearly adsorbed carbonyls appear at around

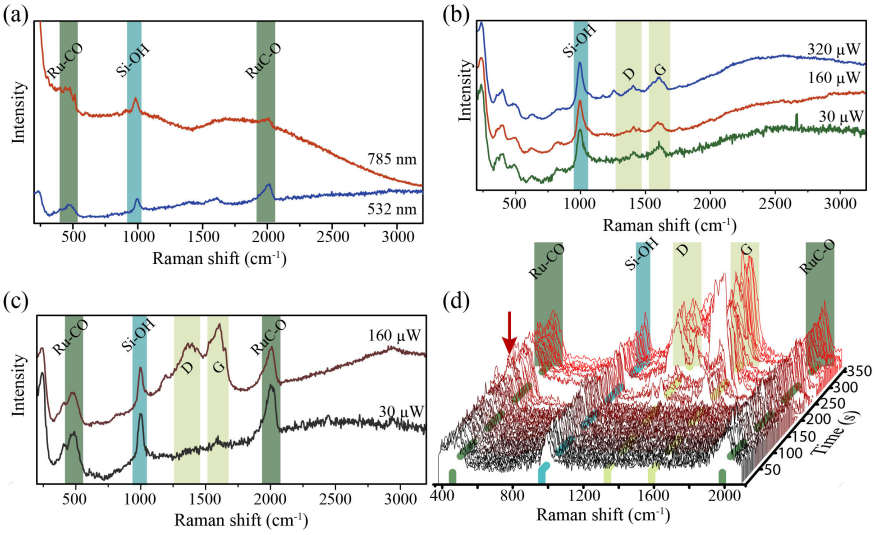

Figure 4. The effect of laser power on the SHINER spectra of Ru/Ag@SiO_2 measured with *in situ* SHINERS: **(a)** Ru/Ag@SiO_2 in CO-rich atmosphere at 150 °C under 10 s, 30 μW, 532 nm (lower, blue line) and 10 s, 1.7 mW, 785 nm (upper, red line) excitation; **(b)** SHINERS measurements on Ru/Ag@SiO_2 in hydrogen atmosphere (50 H_2:40 Ar mL/min at 300 °C) with 30 μW, 160 μW and 320 μW with 10 s integration time. **(c)** SHINERS measurements on Ru/Ag@SiO_2 in methanation conditions (50 H_2:5 CO:40 Ar mL/min at 210 °C) with 30 and 160 μW for 10 s integration time. **(d)** Time-dependent SHINERS measurements on Ru/Ag@SiO_2 in methanation conditions (50 H_2:5CO:40Ar mL/min at 210 °C) over 360 s, with 3 s integration time for each spectrum. After 180 s, the laser power is changed from 30 to 160 μW, as is indicated by the red arrow. The spectra are normalized to the Ru–CO band at 470 cm^{-1}.

respectively 480 and 2000 cm^{-1}. Over time, the signal remains stable with 30 μW incident laser power. As soon as the laser power is increased to 160 μW, a marked growth in the intensity of the D and G graphite Raman bands is observed. The laser power effect can be studied with a 3 s integration time to follow the growth of the D and G band in Figure 4d. When the laser power is switched from 30 to 160 μW, random peaks appear between 1100–1600 cm^{-1} that gradually build up to the known D and G bands. When a new location is measured, we again observe the blinking of various peaks in the spectrum and the rise of the D and G bands. Interestingly, under H_2 at 300 °C after all surface-bound CO has reacted, we can increase the laser power to 360 μW without the observation of any spectral blinking or carbon growth (Figure 4b). This indicates that the cleaning methods are successful, and furthermore, that the cleanliness can be verified simply by increasing the laser power under H_2.

With this work we aimed to provide further insight in the contamination causes of *in situ* SHINERS experiments and put forward a set of practical guidelines to obtain clean substrates. Due to the intense local signal intensity near the plasmonic nanostructures, SHINERS is a technique that will always be prone to contamination. It is therefore of utmost importance to work with clean starting materials and clean reaction materials. However, an optimal SHINERS study should involve the cleaning of the substrate, the gas lines and the reaction products. Therefore, we suggest potential users to start with a heat treatment of at least 200 °C in an oxygen-rich environment. Since the gas lines have to be cleaned as well, a flushing step of all gases should be considered of at least 15 min. Finally, any contaminants during catalysis that may be found in the CO feed should be removed with a filter. The filter may consist of ZnO, Al_2O_3, and activated coal to remove respectively water, carbonyls, and organics. Furthermore, one should be aware of the Raman laser power effects in combination with the plasmonic nanoparticles. Depending on the electromagnetic enhancement of the SHINs, a limited laser power or minimized exposure times to prevent carbon growth should be applied. The signal can then be improved by accumulating multiple points with very short exposure times to minimize local sample heating.[21] When these practical steps are followed, a clean(er) SHINER spectrum will be obtained, which can be applied for catalysis research.

Acknowledgements

We thank the Netherlands Organization for Scientific Research (NWO) and Shell Global Solutions in the framework of the Chemical Innovation Partnership Project (CHIPP) for financial support. Hans Meeldijk (Utrecht University) is thanked for his contributions to the TEM-EDX measurements, Lennart Weber (Utrecht University) is thanked for his contribution to the TGA measurement.

Conflict of Interest

The authors declare no conflict of interest.

Keywords: heterogeneous catalysis · nanoparticles · Raman spectroscopy · surface science · transmission electron microscopy

[1] P. G. Etchegoin, E. C. Le Ru, *Phys. Chem. Chem. Phys.* **2008**, *10*, 6079–6089.
[2] H. Knözinger, *Catal. Today* **1996**, *32*, 71–80.
[3] H. Zhang, C. Wang, H. Sun, G. Fu, S. Chen, Y. Zhang, B. Chen, J. R. Anema, Z. Yang, J. Li, Z. Tian, *Nat. Commun.* **2017**, *8*, 15447.
[4] H. Zhang, X.-G. Zhang, J. Wei, C. Wang, S. Chen, H.-L. Sun, Y.-H. Wang, B.-H. Chen, Z.-L. Yang, D.-Y. Wu, J.-F. Li, Z.-Q. Tian, *J. Am. Chem. Soc.* **2017**, *139*, 10339–10346.
[5] T. Hartman, C. S. Wondergem, N. Kumar, A. Van Den Berg, B. M. Weckhuysen, *J. Phys. Chem. Lett.* **2016**, *7*, 1570–1584.
[6] M. Fleischmann, P. J. Hendra, A. J. McQuillan, *Chem. Phys. Lett.* **1974**, *26*, 163–166.
[7] D. L. Jeanmaire, R. P. van Duyne, *J. Electroanal. Chem. Interfacial Electrochem.* **1977**, *84*, 1–20.
[8] M. G. Albrecht, J. A. Creighton, *J. Am. Chem. Soc.* **1977**, *99*, 5215–5217.
[9] M. Moskovits, *J. Chem. Phys.* **1978**, *69*, 4159–4161.
[10] E. M. van Schrojenstein Lantman, T. Deckert-Gaudig, A. J. G. Mank, V. Deckert, B. M. Weckhuysen, *Nat. Nanotechnol.* **2012**, *7*, 583–586.
[11] Z. Zhang, T. Deckert-Gaudig, P. Singh, V. Deckert, *Chem. Commun.* **2015**, *51*, 3069–3072.
[12] C. T. Williams, A. A. Tolia, H. Y. H. Chan, C. G. Takoudis, M. J. Weaver, *J. Catal.* **1996**, *163*, 63–76.
[13] K. N. Heck, B. G. Janesko, G. E. Scuseria, N. J. Halas, M. S. Wong, *J. Am. Chem. Soc.* **2008**, *130*, 16592–16600.
[14] E. M. van Schrojenstein Lantman, P. de Peinder, A. J. G. Mank, B. M. Weckhuysen, *ChemPhysChem* **2015**, *16*, 547–554.
[15] S. Schlücker, *Angew. Chem. Int. Ed.* **2014**, *53*, 4756–4795; *Angew. Chem.* **2014**, *126*, 4852–4894.
[16] T. Wilke, X. Gao, C. G. Takoudis, M. J. Weaver, *J. Catal.* **1991**, *130*, 62–75.
[17] C. E. Harvey, B. M. Weckhuysen, *Catal. Lett.* **2014**, *145*, 40–57.
[18] J. F. Li, Y. F. Huang, Y. Ding, Z. L. Yang, S. B. Li, X. S. Zhou, F. R. Fan, W. Zhang, Z. Y. Zhou, D. Y. Wu, B. Ren, Z. L. Wang, Z. Q. Tian, *Nature* **2010**, *464*, 392–395.
[19] S.-Y. Ding, J. Yi, J.-F. Li, B. Ren, D.-Y. Wu, R. Panneerselvam, Z.-Q. Tian, *Nat. Rev. Mater.* **2016**, *1*, 16021.
[20] T. Hartman, B. M. Weckhuysen, *Chem. Eur. J.* **2018**, *24*, 3733–3741.
[21] B. S. Yeo, T. Schmid, W. Zhang, R. Zenobi, *Appl. Spectrosc.* **2008**, *62*, 708–713.
[22] T. Kang, S. Hong, Y. Choi, L. P. Lee, *Small* **2010**, *6*, 2649–2652.
[23] S. Linic, U. Aslam, C. Boerigter, M. Morabito, *Nat. Mater.* **2015**, *14*, 567–576.
[24] C. T. Williams, C. A. Black, M. J. Weaver, C. G. Takoudis, *J. Phys. Chem. B* **1997**, *101*, 2874–2883.
[25] C. H. Bartholomew, *Appl. Catal. A Gen.* **2001**, *212*, 17–60.
[26] W. Haiss, N. T. K. Thanh, J. Aveyard, D. G. Fernig, *Anal. Chem.* **2007**, *79*, 4215–4221.
[27] J. F. Li, X. D. Tian, S. B. Li, J. R. Anema, Z. L. Yang, Y. Ding, Y. F. Wu, Y. M. Zeng, Q. Z. Chen, B. Ren, Z. L. Wang, Z. Q. Tian, *Nat. Protoc.* **2013**, *8*, 52–65.
[28] C.-J. Jia, F. Schüth, *Phys. Chem. Chem. Phys.* **2011**, *13*, 2457–2487.
[29] R. L. Craig, A. L. Bondy, A. P. Ault, *Anal. Chem.* **2015**, *87*, 7510–7514.
[30] J. Ofner, T. Deckert-Gaudig, K. A. Kamilli, A. Held, H. Lohninger, V. Deckert, B. Lendl, *Anal. Chem.* **2016**, *88*, 9766–9772.
[31] S. Y. Mar, C. S. Chen, Y. S. Huang, K. K. Tiong, *Appl. Surf. Sci.* **1995**, *90*, 497–504.
[32] G. Gouadec, P. Colomban, *Prog. Cryst. Growth Charact. Mater.* **2007**, *53*, 1–56.
[33] E. V. Formo, Z. Wu, S. M. Mahurin, S. Dai, *J. Phys. Chem. B* **2011**, *115*, 9068–9073.
[34] R. J. Peláez, J. P. Espinós, C. N. Afonso, *Nanotechnology* **2017**, *28*, 175709.
[35] F. Thibault-starzyk, E. Seguin, S. Thomas, M. Daturi, H. Arnolds, D. A. King, *Science* **2009**, *324*, 1048–1051.

[36] P. F. McMillan, R. L. Remmele, *Am. Mineral.* **1986**, *71*, 772–778.
[37] P. Munnik, P. E. De Jongh, K. P. De Jong, *Chem. Rev.* **2015**, *115*, 6687–6718.
[38] L. H. Leung, M. J. Weaver, *Langmuir* **1988**, *4*, 1076–1083.
[39] M. A. Barteau, J. Q. Broughton, D. Menzel, *Surf. Sci.* **1983**, *133*, 443–452.
[40] G. H. Yokomizo, C. Louis, A. T. Bell, *J. Catal.* **1989**, *120*, 1–14.
[41] A. C. Ferrari, *Solid State Commun.* **2007**, *143*, 47–57.
[42] A. M. Ricks, Z. E. Reed, M. A. Duncan, *J. Mol. Spectrosc.* **2011**, *266*, 63–74.
[43] H. Stammreich, K. Kawai, Y. Tavares, P. Krumholz, J. Behmoiras, S. Bril, *J. Chem. Phys.* **1960**, *32*, 1482–1487.
[44] H. Stammreich, K. Kawai, O. S. W. Sala, P. Krumholz, *J. Chem. Phys.* **1961**, *35*, 2168–2174.
[45] R. Smit, C. J. Eijkhoudt, A. J. Van Dillen, J. W. Geus, *Prepr. Pap. Am. Chem. Soc. Div. Fuel Chem.* **1999**, *44*, 119–123.
[46] G. E. Walrafen, M. S. Hokmabadi, N. C. Holmes, *J. Chem. Phys.* **1986**, *85*, 771–776.
[47] E. Smith, G. Dent, *Modern Raman Spectroscopy – A Practical Approach*, John Wiley & Sons, Ltd, Chichester, England, **2005**.

Manuscript received: May 26, 2018
Version of record online: July 11, 2018